

We are IntechOpen, the world's leading publisher of Open Access books Built by scientists, for scientists

6,900

Open access books available

186,000

International authors and editors

200M

Downloads

Our authors are among the

154

Countries delivered to

TOP 1%

most cited scientists

12.2%

Contributors from top 500 universities



WEB OF SCIENCE™

Selection of our books indexed in the Book Citation Index
in Web of Science™ Core Collection (BKCI)

Interested in publishing with us?
Contact book.department@intechopen.com

Numbers displayed above are based on latest data collected.
For more information visit www.intechopen.com



Microscopic Features of Biologically Formed Amorphous Silica

Martin Jensen, Ralf Keding and Yuanzheng Yue
Section of Chemistry, Aalborg University
Denmark

1. Introduction

Many animals base their skeleton on calcium containing compounds and in particular calcium phosphates are prevalent as the main bone constituents. There are, however, animals that rely on different compounds for their skeleton. An example of such a class of animals is sponges, which have a skeleton constituted of silica (Müller et al, 2007). The fact that silica is used as skeleton provides the sponges with the ability to live in calcium-poor and acidic environments. Despite the characteristic composition of the skeleton, sponges have managed to spread to various living environments such as seawater (Bavestrello et al., 1995; Croce et al., 2003; W. E. G. Müller et al., 2005; Pisera, 2003; Schwab & Shore, 1971; Uriz et al., 2000) and lakes (Kaluzhnaya et al., 2005; Schröder et al., 2003). Furthermore, the prevalence of sponge across the entire planet witnesses that they can grow at different temperatures. Due to the unique features of sponges, they have been intensively studied by scientists through the last decades. Many of the studies focused on the evolutionary and biological aspect of sponges (Barthel 1986; Barthel, 1995; Calcinaï et al., 2007). After clarification of the structure of the sponges, it is known that they possess unique features. As a consequence of the unique features of sponges, these creatures have attracted interest from material scientists (Wang et al., 2010) since study of sponges could lead to new materials or facilitate the production of already existing materials through biomimetic approaches.

The composition and structure considerably vary from one type of sponge to another, and therefore it is not possible to address all kinds of sponges in one chapter. In this chapter, we focus on the sponge called *Cauxi* (Porifera, Demospongiae). From its habitat in the lower Rio Negro in the eastern Amazon basin, the natives have known and used the sponge for reinforcement of their pottery through centuries (Costa et al., 2004). Besides the fact that the sponge is known to be amorphous to X-ray diffraction (XRD), the mesoporous feature of the sponge remained unrevealed until recently (Jensen et al., 2009). In this work, we present a detailed description of the fascinating features of the *Cauxi* sponge and highlight differences between *Cauxi* and other species. This work will also shed light on the potential of biological formation of amorphous mesoporous materials at ambient conditions.

2. Materials and methods

2.1 Extraction of the sponge

The freshwater sponge *Cauxi* was collected at the river bank of the Rio Negro at Praia Grande in the Amazon basin 60 km west of Manaus, Brazil (3°03'22.5S and 60°30'33.56W).

After extraction, the sponge was stored in a plastic bag under dry conditions at room temperature. The sponge belongs to the group of Demospongiae, Porifera.

2.2 Bleaching

To separate the inorganic part from the organic part of the sponge, the organic part of the sponge was removed by means of bleaching. A selected amount of the sponge was added to a Teflon container and mixed with 35 % H₂O₂, 69 % HNO₃, and water in the volume ratio 8:7:1. The Teflon container was placed in a 90 °C water bath for 20 min as the heat accelerates the breakdown of organic material. The solvents were then removed and fresh solvents added. The container was replaced in the water bath for 20 min. The procedure was repeated until a white material without any colorants appeared in the Teflon container. The solvents were then removed and the material rinsed once with water. The material was heated at 160 °C for 2h in order to evaporate any remaining bleaching agent without changing the properties of the bleached material.

2.3 Calorimetric measurements

Calorimetric and gravimetric responses of the sponge to temperature were measured using a simultaneous thermal analyzer (NETZSCH STA 449C Jupiter (Selb, Germany)), which provides functions of both differential scanning calorimeter (DSC) and a thermogravimeter. For the measurements, a platinum crucible containing the sample and an empty reference platinum crucible were placed on the sample carrier at room temperature. Initially both crucibles were held 5 minutes at an initial temperature of 333 K. Thereafter an upscan to 1543 K and a subsequent downscan were performed at 10 K/min. The samples underwent a second up- and downscan with 10 K/min in order to achieve uniform thermal histories (Yue, 2008). The purge gas was air with a flow of 40 mL/min. Before measuring each sample, a baseline was measured by using two empty crucibles according to the above-stated heating procedure, which was used for correcting the DSC signal of the samples. The isobaric heat capacity (C_p) of the samples was determined by comparing the heat flow data of the samples with those of a reference sample (sapphire) measured using the above-stated heating procedure, since the temperature dependence of the C_p values of the sapphire is known.

2.4 Heat treatments

To remove the organic material from the inorganic part by another approach than bleaching, a part of the sponge was put in a porcelain crucible and heat-treated in a muffle furnace (Scandiaovnen A/S, Denmark) in air at 823 K for 7 h. This temperature was selected in such manner that all organic substances could be completely removed.

Another sample was prepared by heating untreated sponge in an alumina crucible in air to 1723 K for 17h in an Entech SF6/17 electric furnace (Ängelholm, Sweden) in order for the material to crystallise.

2.5 Scanning electron microscopy (SEM) imaging

SEM measurements were done on a Zeiss 1540 XB scanning electron microscope (Oberkochen, Germany) using uncoated samples. The secondary electrons were recorded using an acceleration voltage of 1 kV. Images of untreated, bleached, and heat treated samples were acquired.

2.6 Transmission electron microscopy (TEM) imaging

Since it was not possible to obtain any images with sufficient contrast on the untreated sponge, heat treated samples were used for transmission electron microscope (TEM) imaging. After annealing the untreated sponge in an electric furnace at 1723 K for 17 h it was finely ground using an agate mortar. The obtained powder was dispersed in isopropanol and after thorough dispersing, a droplet of the dispersion was allowed to dry on a carbon-coated copper grid. The ground, heat-treated sponge fragments kept on the grid were imaged in a high-resolution TEM (JEOL JEM 4010, acceleration voltage 400 keV, point-to-point resolution: 0.155 nm).

2.7 Optical microscopy

The fibres were investigated on a Zeiss Axioskop microscope. The length of the sponge spicules was measured employing a 10x objective. The width was measured as the broadest point of the spicule with a 100x objective in oil immersion. Both width and length measurements were done on 50 spicules.

2.8 X-ray fluorescence

Bleached sponge powder of about 2 grams was mixed with 12 g $\text{Li}_2\text{B}_4\text{O}_7$ per gram powder. The mixture was melted at 1573 K and made into a tablet. The tablet was placed in a sample holder, and after calibration, the measurement was initiated. The measurement was conducted on a S4-Pioneer X-ray spectrometer (Bruker-AXS, Karlsruhe, Germany).

2.9 Vacuum hot extraction

The water content of the bleached fibres was measured by mass spectrometry coupled with vacuum hot extraction. Prior to the measurement, the sample was kept at 473 K to remove adsorbed water. The sample was cooled to room temperature in the device. Subsequently, the degassing rate was recorded upon heating of the sample with a rate of 10 or 20 K/min to 1773 K.

2.10 Small angle X-ray scattering

The small angle X-ray scattering (SAXS) measurements were done on a pinhole instrument. The instrument was a modified version of a commercially available small-angle X-ray camera (NanoStar, Bruker AXS). It employs a rotating anode X-ray source ($\text{CuK}\alpha$) (0.1 x 1.0 mm² source size with a power of 1 kW) and a set of cross-coupled Göbel multilayer mirrors for monochromatising the radiation and for converting the divergent beam from the source to an essentially parallel beam. To reduce the background, the instrument has an integrated vacuum. The instrument covers a range of scattering vectors q between 0.010 and 0.35 Å⁻¹ ($q = (4\pi/\lambda) \sin \theta$, where 2θ is the scattering angle and $\lambda = 1.542$ Å, the X-ray wavelength). All measurements were made at room temperature. The SAXS data were azimuthally averaged, corrected for variations in detector efficiency and for spatial distortions. After the background subtraction, the data is converted to an approximate absolute scale using the scattering from pure water as a primary standard.

For the experiments, a bunch of the thin spicules were collected using a Scotch® tape in such a way that they were randomly oriented. The scattering data of a clean tape was used as background for the data treatment.

2.11 X-ray diffraction

The sample heat-treated at 1723 K was measured with a Seifert FPM HZG4 diffractometer (Freiburg, Germany) with Fe K α radiation. The scan was conducted in the range $5^\circ < 2\theta < 65^\circ$.

3. Results and discussion

3.1 Macroscopic structure of the sponge

The sponge itself has a hard, but somewhat brittle and spherical structure with a brownish colour (Fig. 1). The brown colour arises from the organic part of the organic and from humic acids from the river that have precipitated on the skeleton of the sponge (Keding et al., 2010). The initial key findings of the structure of the sponge are reported in Jensen et al., (2009).



Fig. 1. The *Cauxi* sponge. In the lower right corner, the branch that the sponge was attached to appears.

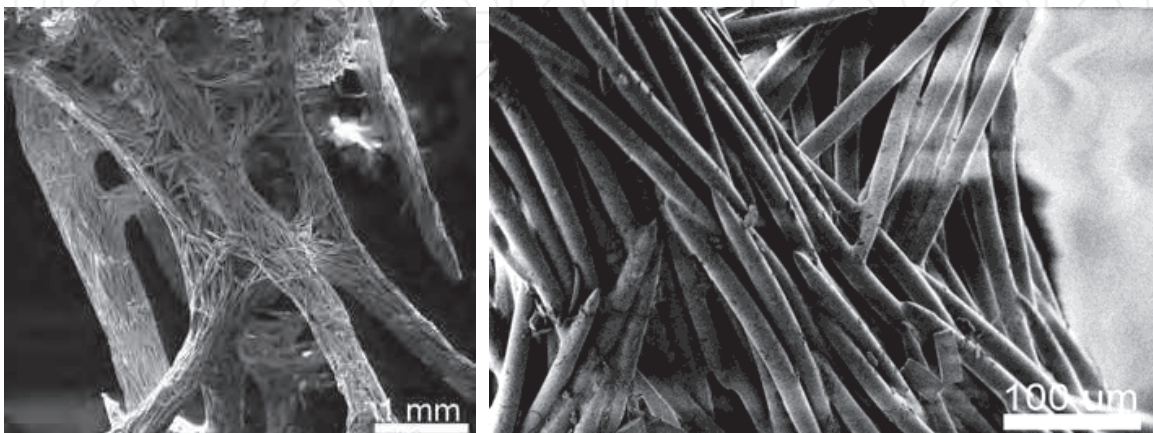


Fig. 2. SEM images of the untreated sponge.

To examine the macroscopic structure of the sponge, scanning electron microscopy (SEM) images are acquired. The skeleton consists of needle shaped spicules that are bundled together (Fig. 2). There are branches on the bundles of spicules which give the sponge its porous structures. Due to the porous structure, the density of the sponge is only about 15 g/L.

When examining each individual spicule, it is seen that spicules are cemented through junctions (Fig. 3a) and that an axial cavity in each spicule exists (Fig 3b).

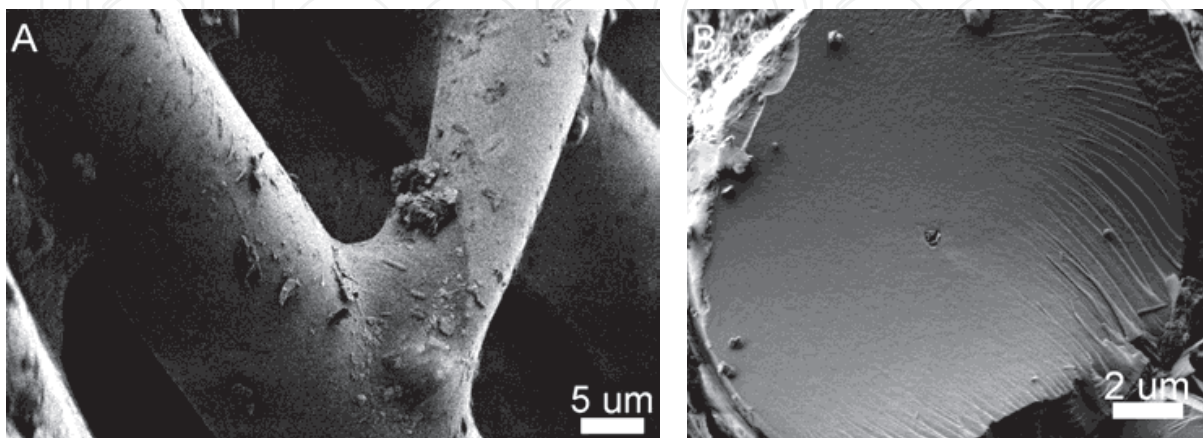


Fig. 3. SEM images of untreated sponge showing junction between two spicules (A) and a cross section of a spicule (B).

The presence of an axial channel in the spicules is a common feature for sponges (Aizenberg et al., 2005; Cha et al., 1999; W. E. G. Müller et al., 2005; Schwab & Shore, 1971, Uriz et al., 2000). The axial channel has been found to harbour an axial filament containing the catalytic protein silicatein (Cha et al., 1999; Shimizu et al., 1998). Furthermore, the cross section of the spicules in Fig. 4B shows a solid structure around the channel, whereas other sponges have a layered structure (Aizenberg et al., 2004; Levi et al., 1989; Shore, 1972; Uriz et al., 2000).

To investigate the chemical nature of the junctions, spicules subjected to bleaching and heat-treatment at 823 K are considered. After the two treatments, the sponge loses its macroscopic structure and appears as a powder. The loss of the macroscopic structure is confirmed by SEM, since only isolated spicules are found (Fig. 4).

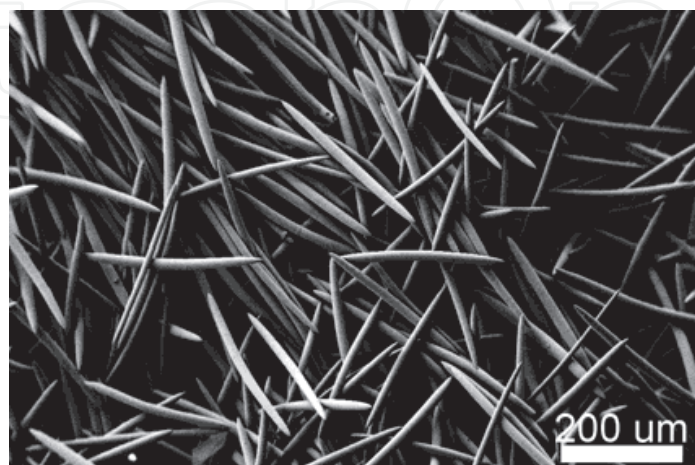


Fig. 4. SEM image of spicules subjected to bleaching.

From Fig. 4 it can be observed that the junctions that cement the spicules have been removed. As a consequence of the removal of the junctions, the macroscopic structure of the sponge collapses and isolated fibres are left. The length and width of the spicules have by optical microscopy been measured to 305 and 15.6 μm , respectively. Since the macroscopic structure collapses after both bleaching and heat treatment at 823 K, it can be concluded that the junction consists of organic material. This is in contrast to spicules in other sponges that are cemented by a silica deposition (Aizenberg et al., 2005). Due to the brittle nature of the spicules, sponges that apply silica cemented spicules, obtain mechanical stability by a hierarchical arrangement (Aizenberg et al., 2005). As *Cauxi* lives in a river with a strong current, *Cauxi* requires a larger flexibility than the sea sponges. In the sponges that cement their spicules by silica depositions, a layered coaxial structure of the spicule is found. Between each of the layer, organic material is present (Aizenberg et al., 2005). Resistance to bending stresses in this inorganic skeleton is obtained since a stress that leads to fracture only breaks a single layer of the spicules. Organic junctions provide a better flexibility than the silica depositions and therefore, the spicules in *Cauxi* can be solid without deteriorating the mechanical properties of the skeleton. Thus by combining the strength of an inorganic skeleton and the flexibility of an organic binder to cement the junctions, *Cauxi* obtains a remarkable macroscopic and microscopic strength. In other words, the brittleness of each individual spicule is compensated by the organic binder that cements the spicules into the sponge skeleton. The importance of combining microscopic and macroscopic features to obtain a strong and stable structure in sponges is described for another sponge elsewhere (Aizenberg et al., 2005). Studies of the structure of sponges can provide inspiration for the development of stronger man-made materials.

3.2 Chemical composition of the spicules

The composition of the bleached sponge has been examined using the vacuum hot extraction (VHE) method up to 1780 K for volatile components such as water and by X-ray fluorescence (XRF) for the remaining inorganic components. During the hot extraction experiments, volatile species liberated from the sample upon heating are detected by means of a mass spectrometer. Prior to the VHE experiments, the sample is kept at 473 K to remove water absorbed to the surface of the spicules since the surface of silica is known to be hygroscopic. The release of water vapour from bleached spicules at two different heating rates is shown in Fig. 5.

The water release occurs at similar temperatures at both 10 and 20 K/min. with a maximum release rate around 900 K. The spectrometer measures roughly an ion current that at 20 K/min is twice of that measured at 10 K/min. The increased ion current is caused by the higher heating rate, i.e., the experiment at 20 K/min only has half of the time to release the water compared to a heating rate of 10 K/min and consequently, the water release is twice as intense. Since the water is released at the same temperatures at different heating rates, the water release is thermodynamically and not kinetically controlled. Through integration of the degassing curve in Fig. 5 and the measurement of a standard, it is possible to determine the water content (R. Müller et al., 2005). From this approach a water content of 5.5 wt % is determined.

The XRF measurement shows that the chemical composition of the bleached spicules is dominated by SiO_2 (Table 1). In addition to the 99.7 wt% SiO_2 , the spicules contain impurities. The impurities are mainly CaO and Al_2O_3 and could arise from sample handling and preparation. After the clarification that the spicules mainly consist of SiO_2 , it is investigated

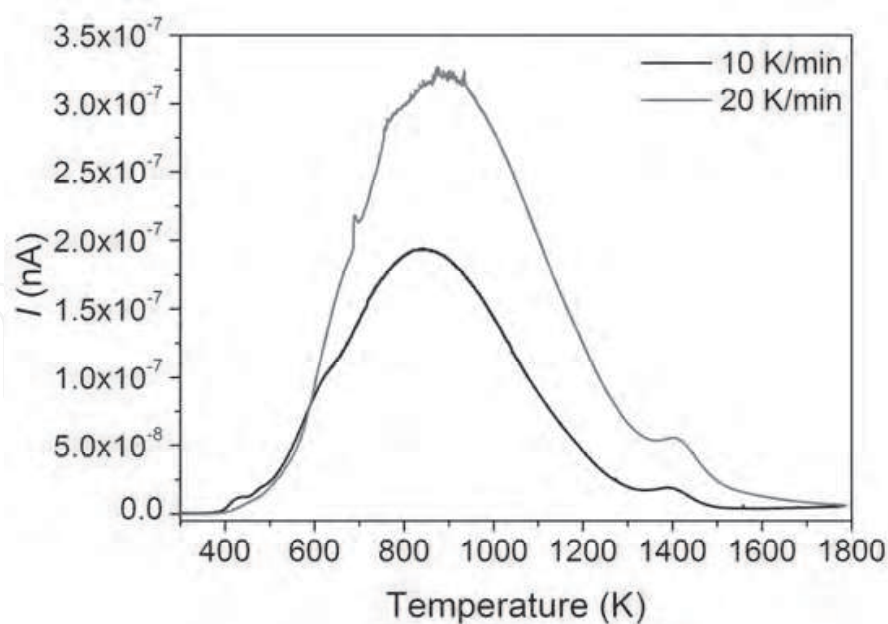


Fig. 5. Ion current as a function of temperature measured at 10 and 20 K/min on bleached spicules. The plotted ion current from the spectrometer is from mass to charge ratio (m/z) 18, i.e., water. The curves have a shoulder at T_g .

	SiO ₂	CaO	SO ₃	Al ₂ O ₃	Fe ₂ O ₃	TiO ₂	K ₂ O	P ₂ O ₅
Content (wt%)	99.7	0.070	0.041	0.07	0.04	0.034	0.010	0.005

Table 1. Chemical composition of the bleached spicules measured by means of XRF.

whether the 5.5 wt% water determined by means of VHE, reside in the glass structure or are present in pores. To do so the glass transition temperature (T_g) is investigated since T_g is affected by water in the glass structure but not water residing in pores isolated from the glassy phase.

3.3 Glass transition temperature

The glass transition temperature (T_g) measured by means of DSC is plotted together with the thermogravimetry signal in Fig. 6. There is an endothermic peak at around 450 K, which is attributed to initial vaporization of superficial water. This is verified by a mass loss in the same temperature region (see the grey curve in Fig. 6). In addition, a broad weak endothermic response is observed at around 1400 K which is a typical feature of the glass transition of the glassy silica. The DSC pattern of untreated sponge is similar to that of the bleached one except for an exothermic peak between 500 and 900 K due to combustion of organic material. The inset in Fig. 6 shows the endothermic event at around 1400 K, where an increase in the heat capacity is clearly seen. This endotherm must be associated with the glass transition of silica (Richet et al., 1982). This implies that the *Cauxi* skeleton is amorphous, which is confirmed by XRD reported elsewhere (Costa et al., 2004). By applying a previously suggested method (Yue, 2008), the T_g of the spicules of the bleached sponge is found to be 1414 K. T_g of silica is very sensitive to hydroxyl groups incorporated in the glass network structure, especially at low concentrations of hydroxyl groups (Deubener

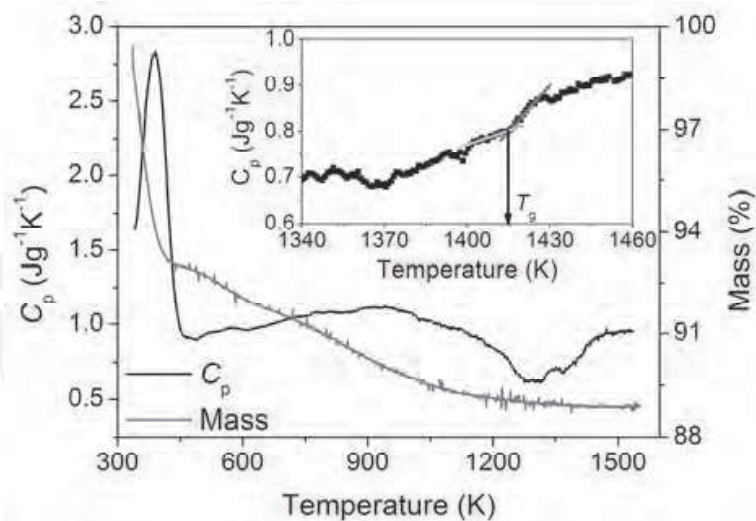


Fig. 6. DSC and TG upscan in air on the bleached sponge. The DSC upscan reveals an initial endothermic peak until around 450 K where the TG curve demonstrates a mass loss. Another endothermic peak occurs in the DSC patterns around 1400 K. Inset: DSC upscan in the range 1300 – 1500 K. The dashed lines in the inset are used to determine T_g .

et al., 2003). To determine the water content in the network structure of the *Cauxi* spicules, it is necessary to know the relationship between T_g and the hydroxyl content in the glass structure. To establish this relationship, the T_g of commercial silica glasses with 1, 150, and 1000 ppm water has been measured and found to be 1438, 1425 and 1375 K, respectively. From the $T_g \sim$ hydroxyl content relationship, it can be interpolated that the spicules of *Cauxi* contain approximately 400 ppm hydroxyl species, i.e., structural water. The large discrepancy between the 400 ppm hydroxyl species determined by means of DSC and the 5.5 wt % determined by VHE, implies that the majority of the water must reside in pores isolated from the glassy network. The exclusion of water from the glass structure is in contrast to other Demospongiae sponges (Sanford, 2003). Since the SEM images in Fig. 2-4 do not reveal the presence of such pores, the water must reside in nanopores or mesopores.

3.4 Mesoporosity

To reveal the presence of possible mesopores, transmission electron microscopy (TEM) and small angle X-ray scattering (SAXS) are employed. Due to pronounced decomposition, TEM images of untreated spicules could not be obtained. Although the bleached spicules underwent massive radiation damage upon TEM inspection, the amorphous nature of the spicules was doubtlessly disclosed. Therefore focus is turned to the sample heat-treated at 1723 K.

The TEM image in Fig. 7 reveal mesoscale crystalline phases (dark areas) embedded in the amorphous phase. The crystalline phases possess a width of ~ 15 nm and a length of up to 200 nm and seem to be randomly orientated in the amorphous phase. To study the crystalline phase a high resolution TEM (HRTEM) image is recorded (Fig. 8).

The HRTEM image in Fig. 8, shows that the crystalline phase indeed is embedded in the amorphous phase. Hence, upon heat treatment at 1723 K, initially causes a removal from some type of mesopores (Fig. 5 and Fig. 6 TG curve) where after a crystallisation of the

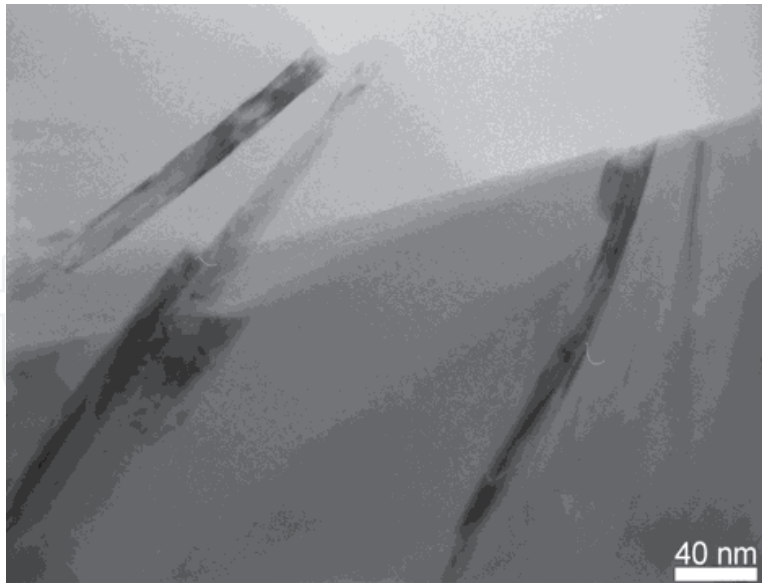


Fig. 7. Bright-field transmission electron micrograph of a spicule after heat-treatment at 1723 K for 17 hours.

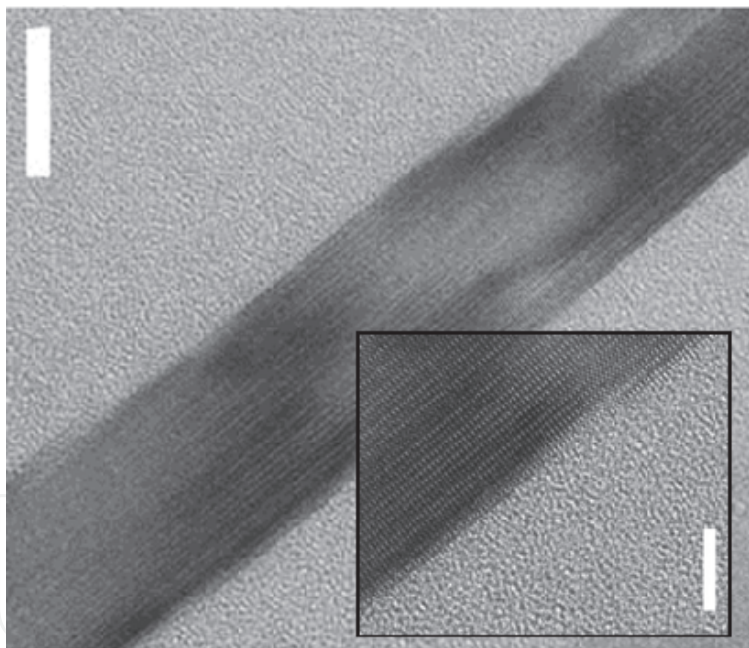


Fig. 8. HRTEM image showing the single channel (scale bar, 20 nm). Inset: Close-up high-resolution transmission electron micrograph (scale bar, 5 nm).

surface layer of the mesopores occurs. The presence of mesopores explains that the water is released from the spicules at very high temperatures (Fig. 5). Thus, we can infer that the *Cauxi* skeleton indeed contains mesopores. Due to surface nucleation effects, the crystallisation occurs more easily at the wall of mesopores than at other places in the bulk part of the spicules. Therefore, only the mesoporous channels and not the bulk of the spicules crystallise. During heat treatment at 1723 K, not only the mesopores, but also the surface of the spicules crystallises (Fig. 9a).

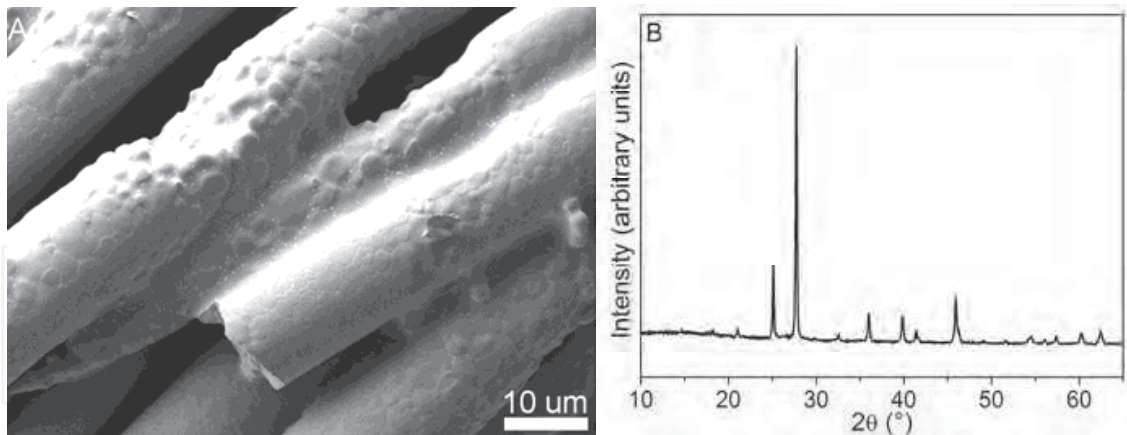


Fig. 9. SEM images of the surface of spicules heat treated at 1723 K (A) and Fe K α XRD pattern of spicules heat treated at 1723 K (B).

On the surface of the spicules, round crystalline structures are found. A comparison with the TEM images in Figs. 7 and 8 shows that only the surface of the fibres and the mesoporous channels crystallise during the heat treatment. X-ray diffraction (XRD) measurements of the heat-treated spicules reveal the presence of cristobalite (Fig. 9B). The presence of cristobalite is expected as it is the stable crystalline form of SiO₂ at high temperatures.

To obtain a fit for the SAXS measurements (Eq. 1) of the untreated spicules, both cylindrical and polymer structures are used (Pedersen, 2000; Pedersen & Gerstenberg, 1996).

$$I = S_{c1}R_{CX}(R, \sigma)P_{ROD}(L) + S_{c1}I_{chain}(R_g) \quad (1)$$

Where S_{c1} and S_{c2} are scale factors for the cylinder and polymer scattering contribution, respectively, σ is the polydispersity of the cylinders, P_{cs} and P_{ROD} are form factors for cross section and length, respectively, and R_g is the radius of gyration for the polymer structure. The Schultz-Zimm distribution is used to calculate the polydispersity. The SAXS measurements and the data fit are given in Fig. 10.

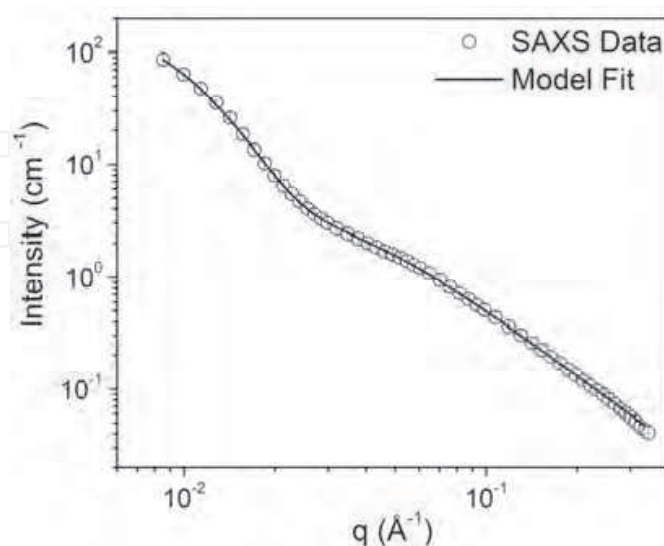


Fig. 10. Small angle X-ray scattering pattern of untreated spicules and the model fit based on Eq. 1.

From the fitting, cylindrical channels with a length and width of 110 and 23 nm, respectively are found. These dimensions correspond well the size of the channels observed on the TEM images in Figs. 7 and 8. Thus the channel like structures detected by SAXS are the mesoporous channels. In addition to the channels, polymer structures with a radius of gyration of 3.45 nm are determined. This polymer structure is expected to be the protein catalysing the polymerisation of silica, i.e, Silicatein. Silicatein has been reported to be similar to Cathepsin S (Shimizu et al., 1998), which has a diameter of 3.0 nm. Since Silicatein contains 50 % more amino acids than Cathepsin, it is likely that Silicatein or an analogue catalytic protein has a radius of gyration of 3.45 nm. Since *Cauxi* excludes water from its siliceous network, *Cauxi* might apply a catalytic protein analogue to Silicatein since sponges with this catalytic protein incorporates water into the silica network.

3.5 Formation of mesoporous amorphous silica

The growth mechanism of *Cauxi* (Jensen et al., 2009) and a review of the growth mechanisms of sponges in general have been described elsewhere (Wang et al., 2010). Here we focus on discussion of the chemical aspects of the formation of pure, mesoporous, amorphous silica and its applications. In order to polymerise silica for its skeleton, *Cauxi* must live in water, which is supersaturated with silica. The supersaturation can arise from pH changes since the lowest solubility of silica in water is around pH 7-8 (Iler, 1979). Hence, if the silica is dissolved in the water (as silicic acids) at a pH with high solubility and a subsequent pH change causes lower silica solubility, the water becomes supersaturated in silica. Despite the supersaturation, silica does not polymerise spontaneously due to an activation energy of 76.6 kJ/mol (Hurd & Marotta, 1940). The catalytical proteins of sponges overcome this activation energy and enable the polymerisation of silica for their skeletons. Through sol-gel synthesis, it is already possible to polymerise silica in water and at ambient temperatures. However, these sol-gel silica glasses contain water in the per cent level in the silica network, which is similar to that of most sponges. Thus, a biomimetic approach of silica must lead to a silica glass with low content of hydroxyl groups in the silica structure. Since *Cauxi* unlike other sponges has been shown to exclude water from the siliceous network of its spicules, studies on *Cauxi* are from this perspective more relevant than studies on sponges with a large content of hydroxyl groups in their silica network. From other sponges, the catalytic proteins have been isolated and expressed in *E. coli*, which is capable of polymerising silica *In vitro* (Cha et al., 1999). A similar approach on *Cauxi* could lead to the production of mesoporous amorphous silica without the incorporation of water into the glass structure since water incorporation weakens the strength and thermal properties of the silica glass.

The technological and scientific importance of glassy silica is demonstrated by its wide applications such as membranes (de Vos & Verweij, 1998), columns (Dai et al., 2003), heat-proof materials (Saito et al., 2000), optical communication fibres (Tong et al., 2003) and catalysts in organic synthesis (Minakata et al., 2004). At present, silica of high purity is often produced by means of fusing (Brückner, 1970; Tohmon et al., 1989) or argon plasma methods (Tohmon et al., 1989). Due to the costly and advanced methods, a biomimetic approach based on the catalytic proteins in *Cauxi* has the potential to revolutionise the production of high purity silica.

4. Summary

Cauxi consists of amorphous silica spicules that are cemented by an organic binder. A detailed study of the spicules reveals that the spicules contain 400 ppm structural water

(hydroxyl groups) in the silica network. In mesopores within the spicules, 5.5 wt % of water is found, i.e., unlike other sponges *Cauxi* excludes water from its silica network that build up its skeleton. Isolation of the proteins catalysing the silica polymerisation in *Cauxi* followed by expression in e.g. *E. Coli* seems to be a feasible route for biomimetic production of high-purity amorphous silica. If *In vitro* production of the mesoporous amorphous silica by host organisms such as *E. Coli* is feasible, the next step is to explore whether the pore size or the pore volume fraction in the spicules can be tailored by varying the synthesis environment or the amino acid sequence of the catalytic proteins. Complete control of the pore structure provides an avenue for the production of highly selective membrane materials.

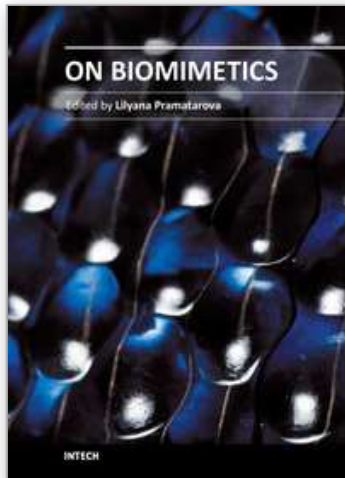
5. References

- Aizenberg, J., Sundar, V. C., Yablon, A. D., Weaver, J. C., Chen, G. (2004). Biological glass fibers: correlation between optical and structural properties. *Proceedings of the National Academy of Sciences of the United States of America*, vol. 101, No. 10, pp. 3358-3363.
- Aizenberg, J., Weaver, J. C., Thanawala, M. S., Sundar, V. C., Morse, D. E., Fratzl, P. (2005). Skeleton of *Euplectella* sp.: Structural hierarchy from the nanoscale to the macroscale. *Science*, vol. 309, No. 5732. Pp. 275-278.
- Barthel, D. (1986). On the ecophysiology of the sponge *Halichondria panicea* in Kiel Bight. I. Substrate specificity, growth and reproduction. *Marine Ecology – Progress Series*, vol. 32, pp. 291-298.
- Barthel, D. (1995). Tissue composition of sponges from the Weddell, Sea, Antarctica: not much meat on the bones. *Marine Ecology – Progress Series*, vol. 123, pp. 149-153.
- Bavestrello, G., Arillo, A., Benatti, U., Carrano, C., Cattaneo-Vietti, R., Cortesogno, L., Gaggero, L., Giovine, M., Tonetti, M., Sarà, M. (1995). Quartz dissolution by the sponge *Chondrosia reniformis* (Porifera, Demospongiae). *Nature*, vol. 378, No. 6555, pp. 374-376.
- Brücker, R. (1970). Properties and structure of vitreous silica. *Journal of Non-Crystalline Solids*, vol. 5, No. 2, pp.123-174.
- Calcinai, B., Cerrano, C., Bavestrello, G. (2007). Three new species and one re-description of *Aka*. *Journal of the Marine Biological Association of the United Kingdom*, vol. 87, No. 6, pp. 1355-1365.
- Cha, J. N., Shimizu, K., Zhou, Y., Christiansen, S. C., Chmelka, B. F., Stucky, G. D., Morse, D. E. (1999). Silicatein filaments and subunits from a marine sponge direct the polymerization of silica and silicones *in Vitro*. *Proceedings of the National Academy of Sciences of the United States of America*, vol. 96, No. 2, pp. 361-365.
- Costa, M. L., Kern, D. C., Pinto, A. H. E., Souza, J. R. T. (2004). The ceramic artifacts in archeological black earth (terra preta) from lower Amazon region, Brazil: Mineralogy. *Acta Amazonica*, vol. 34, No. 2, pp. 165-178.
- Croce, G., Franche, A., Milanese, M., Viterbo, D., Bavestrello, G., Benatti, U., Giovine, M., Amenitsch, H. (2003). Fiber diffraction study of spicules from marine sponges. *Microscopy Research and Technique*, vol. 62, No. 4, pp. 378-381.
- Dai, J., Yang, X., Carr, P. W. (2003). Comparison of the chromatography of octadecyl silane bonded silica and polybutadiene-coated zirconia phases based on a diverse set of cationic drugs. *Journal of Chromatography A*, vol. 1005, No. 1-2, pp.63-82.

- Deubener, J., Müller, R., Behrens, H., Heide, G. (2003). Water and the glass transition of silicate melts. *Journal of Non-Crystalline Solids*, vol. 330, No. 1-3, pp. 268-273.
- de Vos, R. M., Verweij, H. (1998) High-selectivity, high-flux silica membranes for gas separation. *Science*, vol. 279, No. 5357, pp. 1710-1711.
- Hurd, C. B., Marotta, A. J. (1940). Studies of silicic acid gels. The time of set of acidic and basic mixtures containing phosphoric acid. *Journal of Physical Chemistry*, vol. 62, No. 10, , pp. 2767-2770.
- Iler, K. (1979). *The chemistry of silica: Solubility, polymerization, colloid and surface properties, and biochemistry*. John Wiley, 978-0471024040, New York (USA).
- Jensen, M., Keding, R., Höche, T., Yue, Y. Z. (2009). Biologically formed mesoporous amorphous silica. *Journal of the American Chemical Society*, vol. 131, No. 7, 2717-2721.
- Kaluzhnaya, O. V., Belikov, S. I., Schröder, H. C., Rothenberger, M., Zapf, S., Kaandorp, J. A., Borejko, A., Müller, I. M., Müller, W. E. G. (2005). Dynamics of skeleton formation in the lake baikal sponge *Lubomirskia baicalensis*. Part I. Biological and biochemical studies. *Naturwissenschaften*, vol. 92, No. 3, pp. 128-133.
- Keding, R., Jensen, M., Yue, Y. Z. (2010). Characterization of the mesoporous amorphous silica in the fresh water sponge *Cauxi*. *Ceramic Transactions*, vol. 212, pp. 114-120.
- Levi, C., Barton, J. L., Guillemet, C., Le Bras, E., Lehuede, P. (1989). A Remarkably Strong Natural Glassy Rod: The Anchoring Spicule of the *Monorhaphis* Sponge. *Journal of Materials Science Letters*, vol. 8, No. 3, pp. 337-339.
- Minakata, S., Kano, D., Oderaotoshi, Y., Komatsu, M. (2004). Silica-water reaction media: its application to the formation and ring opening of aziridines. *Angewandte Chemie International Edition*, vol. 43, No. 1, pp. 79-81.
- Müller, R., Gottschling, P., Gaber, M. (2005). Water concentration and diffusivity in silicates obtained by vacuum extraction. *Glass Science and Technology*, vol. 78, No. 2, pp.76-89.
- Müller, W. E. G., Li, J. H., Schröder, H. C., Qiao, L., Wang, X. H. (2007). The unique skeleton of siliceous sponges (Porifera; Hexactinellida and Demospongiae) that evolved first from the Urmetazoa during the Proterozoic: a review. *Biogeosciences*, vol. 4, No. 2, pp. 219-232.
- Müller, W. E. G., Rothenberger, M., Boreiko, A., Tremel, W., Reiber, A., Schröder, H. C. (2005). Formation of siliceous spicules in the marine demosponge *Suberites domuncula*. *Cell & Tissue Research*, vol. 321, No. 2, pp. 285-297.
- Pedersen, J. S. (2000). Form factors of block copolymer micelles with spherical, ellipsoidal and cylindrical cores. *Journal of Applied Crystallography*, vol. 33, No. 3, pp. 637-640.
- Pedersen, J. S., Gerstenberg, M. C. (1996) Scattering form factor of block copolymer micelles. *Macromolecules*, vol. 29, No. 4, pp. 1363-1365.
- Pisera, A. (2003). Some aspects of silica deposition in lithistid demosponge *Desmas*. *Microscopy Research and Technique*, vol. 62, No. 4, pp. 312-326.
- Richet, P, Bottinga, Y., Denielou, L., Petitet, J. P., Tequi, C. (1982). Thermodynamic properties of quartz, cristobalite and amorphous SiO₂: drop calorimetry measurements between 1000 and 1800 K and a review from 0 to 2000 K. *Geochimica et Cosmochimica Acta*, vol. 46, No. 12, pp. 2639-2658.
- Saito, K. Ogawa, N., Ikushima, A. J., Tsurita, T., Yamahara, K. (2000). Effects of aluminium impurity on the structural relaxation of silica. *Journal of Non-Crystalline Solids*, vol. 270, No.1-3, pp. 60-65.

- Sandford, F. (2003). Physical and chemical analysis of the siliceous skeletons in six sponges of two groups (Demospongiae and Hexactinellida). *Microscopy Research and Technique*, vol. 62, No. 4, 336-355.
- Schröder, H. C., Efremova, S. M., Itskovich, V. B., Belikov, S., Masuda, Y., Krasko, A., Müller, I. M., Müller, W. E. G. (2003). Molecular phylogeny of the freshwater sponges in lake Baikal. *Journal of Zoological Systematics and Evolutionary Research*, vol. 41, No. 2, pp. 80-86.
- Schwab, D. W., Shore, R. E. (1971). Fine structure and composition of a siliceous sponge spicule. *Biological Bulletin*, vol. 140, No. 1, 125-136.
- Shimizu, K., Cha, J., Stucky, G. D., Morse, D. E. (1998). Silicatein α : Cathepsin L-like protein in sponge biosilica. *Proceedings of the National Academy of Sciences of the United States of America*, vol. 95, No. 11, pp. 6243-6238.
- Shore R. E. (1972). Axial filament of silicious sponge spicules, its organic components and synthesis. *Biological Bulletin*, vol. 143, No. 3, pp. 689-698.
- Tohmon, R., Shimogaichi, Y., Mizuno, H., Ohki, Y., Nagasawa, K., Hama, Y. (1989). 2.7-eV luminescence in as-manufactured high-purity silica glass. *Physical Review Letters*, vol. 62, No. 12, pp. 1388-1391.
- Tong, L. M., Gattass, R. R., Ashcom, J. B., He, S. L., Lou, J. G., Shen, M., Maxwell, I., Mazur, E. (2003). Subwavelength-diameter silica wires for low-loss optical wave guiding. *Nature*, vol. 426, No. 6968, pp. 816-819.
- Uriz, M. J., Turon, X., Becerro, M. A. (2000). Silica deposition in Demosponges: spiculogenesis in *Crambe crambe*. *Cell & Rissue Research*, vol. 301, No. 2, pp. 299-309.
- Wang, X. H., Wiens, M., Schröder, H. C., Hu, S. X., Mugnaioli, E., Kolb, U., Tremel, W., Pisignano, D., Müller, W. E. G. (2010). Morphology of sponge spicules: Silicatein a structural protein for bio-silica formation. *Advanced Biomaterials*, vol. 12, No. 9, pp. B422-B437.
- Yue, Y. Z. (2008). Characteristic temperatures of enthalpy relaxation in glass. *Journal of Non-Crystalline Solids*, vol. 354, No. 12-13, pp. 1112-1118.

IntechOpen



On Biomimetics

Edited by Dr. Lilyana Pramatarova

ISBN 978-953-307-271-5

Hard cover, 642 pages

Publisher InTech

Published online 29, August, 2011

Published in print edition August, 2011

Bio-mimicry is fundamental idea –How to mimic the Nature™ by various methodologies as well as new ideas or suggestions on the creation of novel materials and functions. This book comprises seven sections on various perspectives of bio-mimicry in our life; Section 1 gives an overview of modeling of biomimetic materials; Section 2 presents a processing and design of biomaterials; Section 3 presents various aspects of design and application of biomimetic polymers and composites are discussed; Section 4 presents a general characterization of biomaterials; Section 5 proposes new examples for biomimetic systems; Section 6 summarizes chapters, concerning cells behavior through mimicry; Section 7 presents various applications of biomimetic materials are presented. Aimed at physicists, chemists and biologists interested in biomineralization, biochemistry, kinetics, solution chemistry. This book is also relevant to engineers and doctors interested in research and construction of biomimetic systems.

How to reference

In order to correctly reference this scholarly work, feel free to copy and paste the following:

Martin Jensen, Ralf Keding and Yuanzheng Yue (2011). Microscopic Features of Biologically Formed Amorphous Silica, On Biomimetics, Dr. Lilyana Pramatarova (Ed.), ISBN: 978-953-307-271-5, InTech, Available from: <http://www.intechopen.com/books/on-biomimetics/microscopic-features-of-biologically-formed-amorphous-silica>

INTECH
open science | open minds

InTech Europe

University Campus STeP Ri
Slavka Krautzeka 83/A
51000 Rijeka, Croatia
Phone: +385 (51) 770 447
Fax: +385 (51) 686 166
www.intechopen.com

InTech China

Unit 405, Office Block, Hotel Equatorial Shanghai
No.65, Yan An Road (West), Shanghai, 200040, China
中国上海市延安西路65号上海国际贵都大饭店办公楼405单元
Phone: +86-21-62489820
Fax: +86-21-62489821

© 2011 The Author(s). Licensee IntechOpen. This chapter is distributed under the terms of the [Creative Commons Attribution-NonCommercial-ShareAlike-3.0 License](#), which permits use, distribution and reproduction for non-commercial purposes, provided the original is properly cited and derivative works building on this content are distributed under the same license.

IntechOpen

IntechOpen